Volume 15
Number 48
28 December 2024
Pages 20075–20592

Chemical Science

rsc.li/chemical-science

ISSN 2041-6539

ROYAL SOCIETY OF CHEMISTRY

EDGE ARTICLE

Zihao Guo, Jieping Wang, Wenbin Yi *et al.*
Direct synthesis of *N*-perfluoro-*tert*-butyl secondary amines from *N*-trifluoromethyl secondary amines

Chemical Science

ROYAL SOCIETY OF CHEMISTRY

EDGE ARTICLE

View Article Online
View Journal | View Issue

Cite this: *Chem. Sci.*, 2024, **15**, 20171

All publication charges for this article have been paid for by the Royal Society of Chemistry

Received 19th September 2024
Accepted 30th October 2024

DOI: 10.1039/d4sc06335j

rsc.li/chemical-science

Direct synthesis of *N*-perfluoro-*tert*-butyl secondary amines from *N*-trifluoromethyl secondary amines†

Leibing Wang,[a] Zhongyu Feng,[a] Zhen Luo,[a] Zihao Guo,*[a] Jieping Wang*[a] and Wenbin Yi*[ab]

N-Perfluoro-*tert*-butyl (*N*-PF*t*B) secondary amines, harboring a unique ^{19}F-reporting moiety linked directly to nitrogen, are highly attractive due to their diverse potential applications. However, their mild and facile synthesis remains a significant challenge. Herein, we present a safe and efficient strategy for the direct synthesis of *N*-perfluoro-*tert*-butyl secondary amines from readily available *N*-trifluoromethyl secondary amines. Experiments and theoretical calculations demonstrate that this novel protocol encompasses three main processes: the elimination of hydrogen fluoride from the *N*-trifluoromethyl precursor, consecutive addition–elimination conversion of difluoromethyl imine (R–N=CF_2) to hexafluoropropyl imine (R–N=$C(CF_3)_2$), and final addition of R–N=$C(CF_3)_2$ with the *in situ* generated fluoroform (HCF_3). Key advantages of this reaction include the utilization of a single trifluoromethyl source and the *N*-trifluoromethyl starting material itself as the hydrogen source. Notably, the elimination of hydrogen fluoride, facilitated by CsF, is critical for the success of this approach. This method is compatible with a broad range of functional groups, including heterocyclic compounds. ^{19}F MRI experiments suggest promising prospects for PF*t*B-labeled secondary amines as ^{19}F MRI contrast agents.

Introduction

Fluorine chemistry has seen significant advancements in recent years, with applications emerging in biomedicine[1,2] and materials science.[3,4] Synthetic methods for mono-, di-, and trifluoromethylation are now well-established and highly sophisticated.[5] Alongside these developments, short-chain perfluoroalkylation methodologies have garnered increasing attention due to the unique properties of perfluoroalkyl-containing compounds,[6–10] which hold considerable promise in therapeutic and diagnostic applications.[11–13] Perfluoro-*tert*-butyl (PF*t*B) is particularly valuable in this context, playing a crucial role in ^{19}F-labeled NMR[9,14] and MRI probes,[15–17] as well as ^{19}F MRI contrast agents.[18,19] PF*t*B offers a distinct and singular ^{19}F signal, providing significant advantages in imaging. Not only does ^{19}F sensitivity rival that of ^{1}H, but its signal originates solely from the imaging agent, eliminating interference from background signals. Evidently, the growing demand for perfluorinated compounds in these fields underscores the importance of methodological studies for PF*t*B group synthesis.

Given the ubiquitous role of nitrogen in drug molecules, compounds combining nitrogen with the PF*t*B group, particularly *N*-PF*t*B secondary amines, are highly attractive and hold significant promise. However, the lack of a general synthesis method has resulted in limited reports of such compounds to date. The existing route developed by Petrov involves obtaining R–NHC$(CF_3)_3$ from the hexafluoropropyl imine intermediate (R–N=$C(CF_3)_2$) following addition and hydrochloric acid treatment.[20] This intermediate is typically derived from conventional reactions involving gaseous hexafluoroacetone with aromatic primary amines or isocyanates (Fig. 1A).[21,22] However, these procedures suffer from some drawbacks, including the use of highly toxic gases, multiple steps, and demanding operations,[23–25] which significantly hinder the exploration and application of these compounds. Therefore, overcoming these challenges and developing a general strategy for the safe and efficient construction of *N*-PF*t*B secondary amines is critical.

To the best of our knowledge, the conversion from difluoromethyl imine (R–N=CF_2) to hexafluoropropyl imine (R–N=$C(CF_3)_2$) remains unreported. We propose this conversion as a significantly safer and more efficient approach for constructing multi-CF_3 amines, eliminating the need for highly toxic gases. Our strategy leverages a readily available *N*-CF_3 secondary

[a]*School of Chemistry and Chemical Engineering, Nanjing University of Science and Technology, Nanjing 210094, China. E-mail: zihao_guo@njust.edu.cn; jieping.wang@njust.edu.cn; yiwb@njust.edu.cn*

[b]*Key Laboratory of Organofluorine Chemistry, Shanghai Institute Organic Chemistry, Chinese Academy of Sciences, Shanghai 200032, China*

† Electronic supplementary information (ESI) available: Further details of the experimental procedure, ^{1}H, ^{13}C{^{1}H} and ^{19}F{^{1}H} NMR, HPLC spectra, X-ray crystallographic data for **11**. CCDC 2256453. For ESI and crystallographic data in CIF or other electronic format see DOI: https://doi.org/10.1039/d4sc06335j

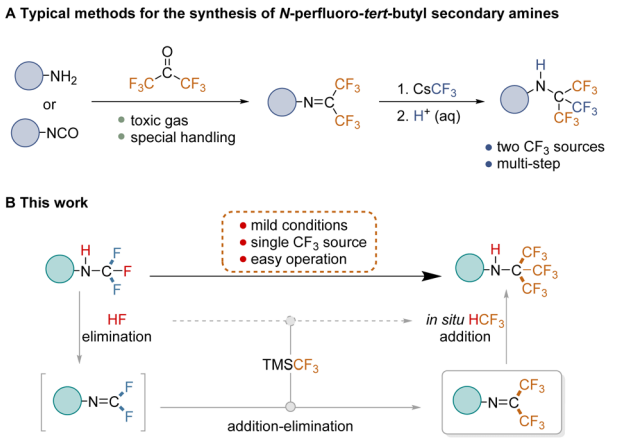

Fig. 1 Previous work and reaction design. (A) Traditional approaches to synthesizing *N*-PF*t*B secondary amines; (B) our designed strategy for the construction of *N*-PF*t*B secondary amines.

amine as the starting material.[26] This amine undergoes elimination of HF to generate the highly reactive difluoromethyl imine. Subsequently, in the presence of a CF_3 source, this imine undergoes two consecutive addition–elimination processes to form hexafluoropropyl imine. Finally, the target *N*-PF*t*B secondary amine is obtained through the addition reaction of hexafluoropropyl imine with trifluoromethyl and hydrogen (Fig. 1B). Experimental and theoretical calculations support the notion that the eliminated HF reacts further with $TMSCF_3$, *in situ* producing HCF_3 which subsequently participates in the addition reaction with hexafluoropropyl imine. The key advantages of this novel strategy lie in its reliance on a single CF_3 source and the starting material *N*-CF_3 secondary amine as the hydrogen source, enabling a one-step reaction under mild conditions.

Results and discussion

To evaluate the proposed reaction pathway, we employed 4-cyanophenyl *N*-trifluoromethyl secondary amine as a model substrate. The substrate was treated with 8.0 equivalents of $TMSCF_3$ and 1.0 equivalent of KF initiator in THF at room temperature for 6 hours. The desired product (compound **1**) was isolated in a 33% yield (Table 1, entry 1). Subsequent attempts to improve the yield by individually or concurrently increasing the amounts of $TMSCF_3$ or KF resulted in only modest improvement. Similarly, the addition of CuCl exhibited a negligible effect on the yield (entries 2–6). Notably, the absence of KF or its substitution with NaF or TBAF (tetrabutylammonium fluoride) completely ablated product formation (entries 7–9). Further investigation revealed that cesium fluoride (CsF) was crucial for this reaction system. When 8.0 equivalents of $TMSCF_3$ were combined with 1.0 equivalent of CsF in the presence of the substrate, the yield remarkably increased to 65% (entry 10). Employing 1.5 equivalents of CsF led to a further enhancement in product yield (entry 11). However, increasing the CsF amount to 3.0 equivalents resulted in an inhibitory effect (increase in unknown by-products, entry 12). Likewise,

Table 1 Survey of reaction conditions[a]

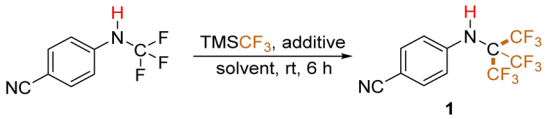

Entry	$TMSCF_3$ (equiv.)	Additive (equiv.)	Solvent	Yield[b] (%)
1	8	KF (1)	THF	33
2	8	KF (3)	THF	38
3	8	KF (5), CuCl (1.0)	THF	54
4	8	KF (3), CuCl (1.0)	THF	47
5	10	KF (5)	THF	43
6	10	KF (3)	THF	42
7	8	—	THF	0
8	8	NaF (3.0)	THF	0
9	8	TBAF (3.0)	THF	0
10	8	CsF (1.0)	THF	65
11	8	CsF (1.5)	THF	73
12	8	CsF (3.0)	THF	67
13	8	CsF (0.5)	THF	60
14	8	CsF (1.5)	DCM	23
15	8	CsF (1.5)	MeCN	41
16	**6**	**CsF (1.5)**	**THF**	**76**
17	10	CsF (3.0)	THF	57

[a] Reaction conditions: *N*-CF_3 secondary amine (0.8 mmol, 1.0 equiv.), solvent (4.0 mL). [b] Isolated yields.

decreasing the CsF quantity to 0.5 equivalents yielded a slightly lower product formation (generation of a dimer, entry 13) (see ESI, p. S4†). These observations collectively suggest that the liberated F^- anion, after being displaced by CF_3^- during the reaction, participates again by reacting with $TMSCF_3$ to release another CF_3^-. Among the tested solvents, THF provided the most favorable outcome (entries 14–15). Finally, the optimal reaction conditions were established by finetuning the ratio of $TMSCF_3$ and CsF (entry 16).

To elucidate the reaction mechanism, we initially employed the *N*-CH_3 analog of the starting substrate under standard conditions (Fig. 2A). This experiment aimed to preliminarily

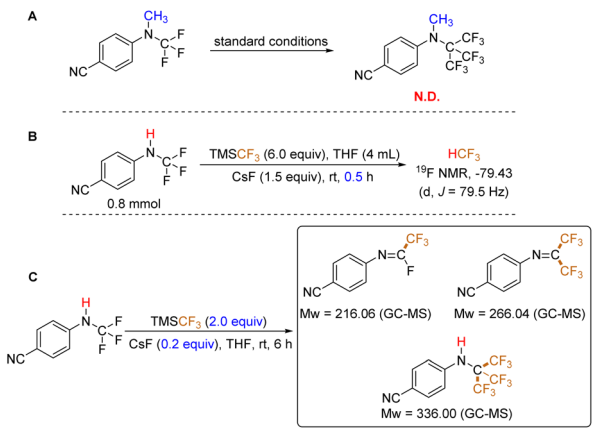

Fig. 2 Preliminary mechanistic investigations.

determine the reaction pathway. Notably, no signal corresponding to the anticipated product was detected by GC-MS or ^{19}F NMR analysis. This observation suggests that the N–H bond in the *N*-CF_3 secondary amine plays a critical role in the reaction, and a simple conversion of the three C–F bonds to C–CF_3 bonds is not the operative mechanism. Secondly, the presence of a fluoroform (HCF_3)[27] signal was identified in the ^{19}F NMR spectrum after 30 minutes of reaction time (Fig. 2B), although a very small amount of HCF_3 is formed in the absence of substrate (see ESI, p. S7†). This finding implies the potential involvement of HF elimination during the reaction. Finally, we investigated the reaction under conditions employing a catalytic amount of CsF (0.2 equivalents) and 2.0 equivalents of $TMSCF_3$ (Fig. 2C). Using GC-MS analysis, we observed a mixture of mono-, di-, and tri-substituted trifluoromethylated products (see ESI, p. S9†).

Density Functional Theory (DFT) calculations were employed to investigate the reaction mechanism (detailed in the ESI, p. S12†). The mechanism can be broadly divided into three key processes: firstly, CsF facilitates the removal of hydrogen fluoride (HF), forming $CsHF_2$; secondly, two sequential addition–elimination processes occur, transforming C–F bonds into C–CF_3 bonds; and finally, the resulting intermediate reacts with the *in situ* generated fluoroform (HCF_3) at the N=C double bond, restoring the hydrogen atom to its original position. The reaction energy barrier diagram is presented in Fig. 3. The DFT calculations reveal that CsF promotes the initial HF elimination process by forming intermediate **IM-1** (−12.2 kcal mol^{-1}) with a significantly lower energy barrier compared to direct HF elimination (kinetic barrier $\Delta G^{\ddagger}_{IM1} = 47.3$ kcal mol^{-1}, thermodynamic barrier $\Delta G^{\circ}_{IM1} = 5.9$ kcal mol^{-1}). Additionally, CsF exhibits a more favorable free energy change ($\Delta G^{\circ}_{CsF} = -12.2$ kcal mol^{-1}) for intermediate formation compared to that of the generation of the intermediate **IM-1** *via* KF ($\Delta G^{\circ}_{KF} = -11.4$ kcal mol^{-1}), underscoring its superior performance in the reaction. CsF reacts with $TMSCF_3$ to form $CsCF_3$, which then attacks **IM-1** and undergoes an addition reaction to form **IM-2** (−51.8 kcal mol^{-1}). Subsequently, **IM-2** undergoes *β*-fluoride elimination, losing one molecule of CsF to give **IM-3** (−49.3 kcal mol^{-1}), introducing the first CF_3 group. Double trifluoromethyl-substituted **IM-5** (−82.8 kcal mol^{-1}) is formed after two consecutive processes. Notably, the $CsHF_2$ formed during the generation of **IM-1** reacts with $TMSCF_3$ to afford HCF_3 ($\Delta G^{\circ}_{Fluoroform} = -18.2$ kcal mol^{-1}), contributing to the exothermic free energy change in the reaction. Finally, the addition reaction of **IM-5** with HCF_3 produces the target product **1**. Importantly, the calculations show that directly eliminating one HF using two CsF equivalents is energetically unfavorable.

We evaluated the applicability of this method to various substrates under the optimized conditions (Table 2). The results reveal a clear influence of the electronic nature of the aryl ring on reaction efficiency. *N*-Trifluoromethyl secondary amines bearing electron-withdrawing groups, similar to the template substrate, yielded the corresponding trifluoromethylated products in good yields (*e.g.*, trifluoromethyl (**2**), nitro (**3**), ester (**4**)).

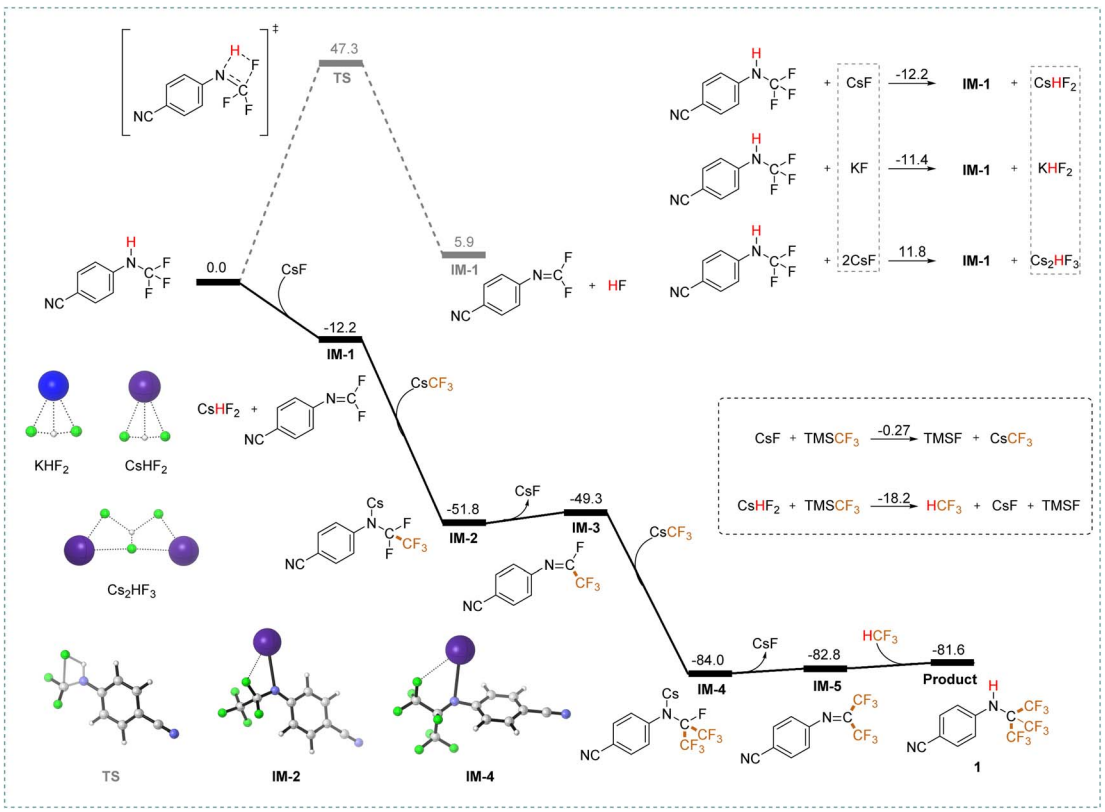

Fig. 3 DFT study on the reaction mechanism.

Table 2 Scope of *N*-perfluoro-*tert*-butyl secondary amines[a]

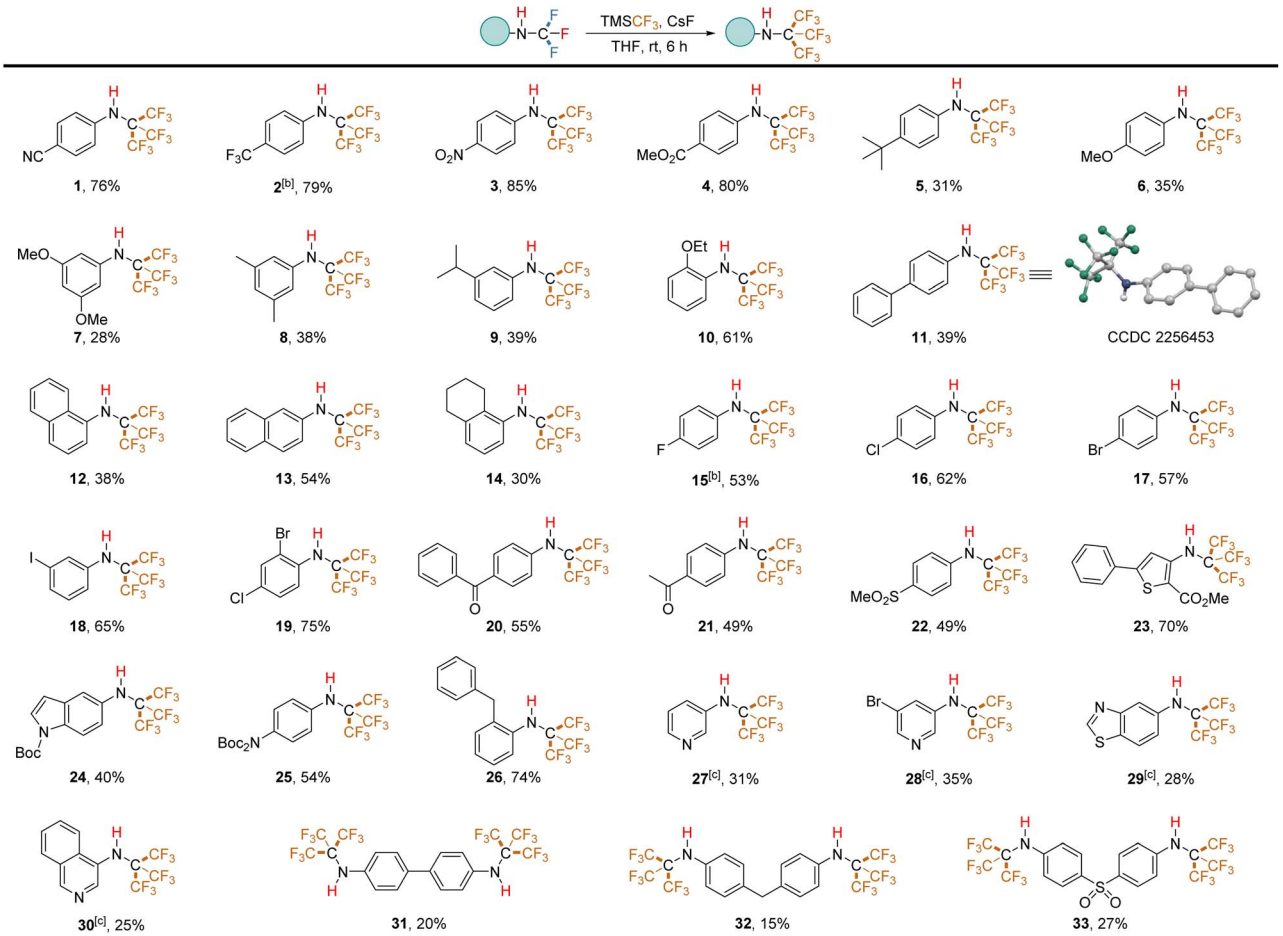

[a] Reaction conditions: *N*-CF_3 secondary amine (0.8 mmol, 1.0 equiv.), $TMSCF_3$ (4.8 mmol, 6.0 equiv.), CsF (1.2 mmol, 1.5 equiv.), THF (4.0 mL), r.t., 6 h. Isolated yields are given. [b] Determined by ^{19}F NMR spectroscopy using trifluoromethoxybenzene as an internal standard. [c] Yield of two steps.

Conversely, electron-rich aromatic rings exhibited lower tolerance. Substrates with *tert*-butyl (**5**), methoxy (**6**, **7**), methyl (**8**), and isopropyl (**9**) groups afforded *N*-PF*t*B secondary amines in lower to moderate yields. Unexpectedly, the *ortho*-ethoxy-substituted compound (**10**) produced the resulting product in a 61% yield. The naphthalene ring was also compatible, although α-naphthalene (**12**) displayed lower reactivity compared to β-naphthalene (**13**), while tetrahydronaphthalene (**14**) showed reactivity akin to that of α-naphthalene, possibly due to steric hindrance from the PF*t*B group. Notably, the presence of fluorine (**15**), chlorine (**16**), bromine (**17**), and iodine (**18**) substituents on the benzene ring did not affect the reaction. These halogens remained intact, as confirmed by the absence of additional trifluoromethyl signals in GC-MS and ^{19}F NMR spectra. This compatibility is advantageous for downstream derivatization reactions. It's important to note that highly fluorinated molecules have a nonpolar character and an extremely low polarizability, inducing only weak intra- and intermolecular interactions.[28] Consequently, substrates **2** and **15**, which contain fluorine and trifluoromethyl groups on the benzene ring, exhibit lower boiling points compared to the other substrates, making it difficult to isolate compounds **2** and **15** under reduced pressure for extended periods. Moderate yields were obtained for ketone substrates (**20**, **21**) and the sulfone substrate (**22**). Perfluoro-*tert*-butylation of thiophene (**23**) and protected nitrogen compounds (**24**, **25**) also proceeded successfully. However, pyridine and thiazole starting materials did not convert to PF*t*B amines under standard conditions, potentially due to the instability of their *N*-CF_3 secondary amine precursors in the solvent-free environment. Optimized conditions were developed for a one-pot conversion of isothiocyanates to *N*-PF*t*B pyridine derivatives (**27**, **28**) in THF (details in ESI, p. S27†). Similarly, trifluoromethylated thiazole (**29**) and isoquinoline (**30**) precursors, synthesized in MeCN but THF instead of Et_2O in the purification procedure, were successfully transformed to corresponding compounds. The synthesis of bis-NHC$(CF_3)_3$-substituted substrates (**31**–**33**) yielded low product quantities. Notably, the standard protocol is not suitable for aliphatic substrates. The structure of *N*-PF*t*B secondary amine **11** was confirmed by X-ray crystallographic

Table 3 Late-stage applications[a]

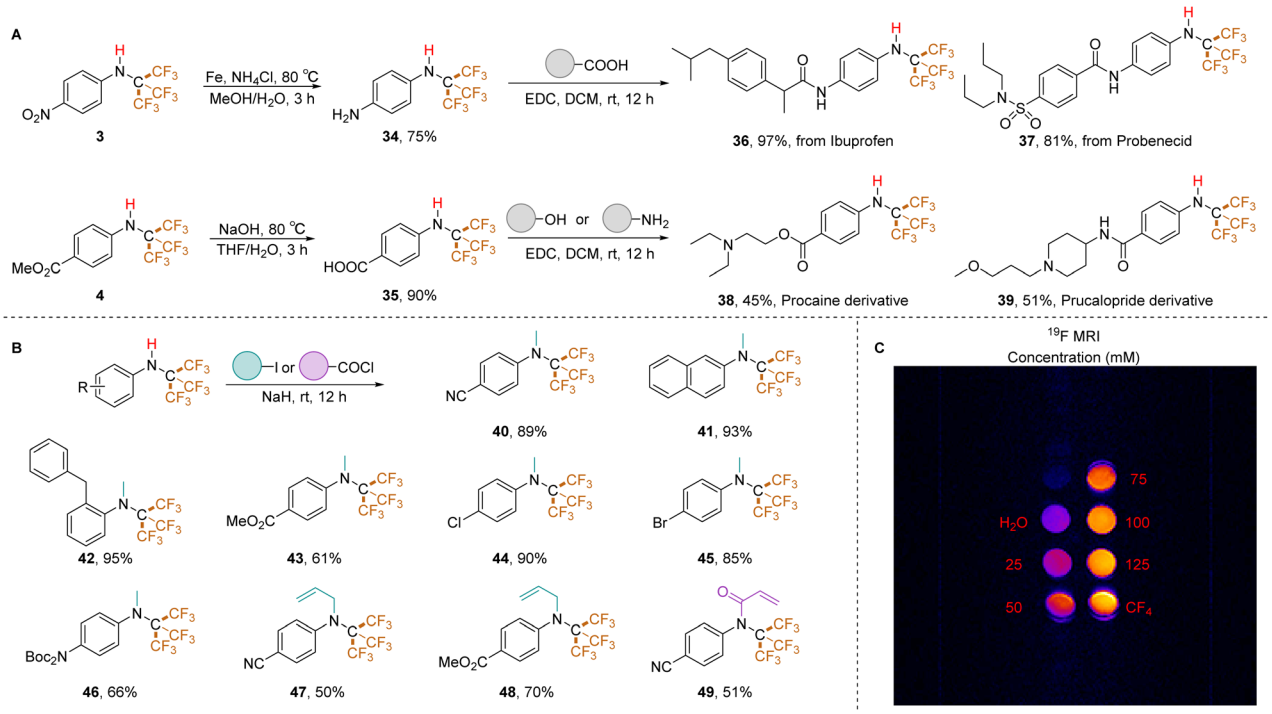

[a] Derivatization and applications of *N*-PF*t*B secondary amines. (A) Synthesis of drug-like molecules (for details, see ESI). (B) Amine (0.3 mmol, 1.0 equiv.), iodide (5.0 equiv.), NaH (10.0 equiv.), THF, r.t., 12 h. (C) MR imaging of ^{19}F at ultra-high field.

analysis. Compound **1** exhibited stability under acidic (aqueous HCl, pH 0, 36 hours) conditions, with no degradation observed by ^{1}H NMR (phenyl region). However, minimal decomposition was detected under basic conditions (aqueous NaOH, pH 14, 36 hours) (details in ESI, p. S42†). The predicted Log *P* value of compound **1** (Log *P* = 4.85) is significantly higher than its *N*-*tert*-butyl counterpart (Log *P* = 2.27), indicating a substantial increase in lipophilicity due to the CF_3 groups.[29]

To assess the utility of this method for incorporating PF*t*B groups into drug-like molecules, we targeted ibuprofen (antipyretic/analgesic) and probenecid (antigout). Since *N*-CF_3 secondary amines bearing an unprotected NH_2 group were not accessible using our previously reported method,[26] it is more feasible to obtain such an active precursor (**34**) by reducing a NO_2 group containing *N*-PF*t*B secondary amine (**3**). Following the reduction of compound **3** and subsequent condensation, the PF*t*B group was successfully introduced into these drugs with excellent yields (ibuprofen: **36**, 97%; probenecid: **37**, 81%). Notably, the PF*t*B group remained intact during ester deprotection. Furthermore, *N*-PF*t*B derivatives of procaine (local anesthetic, **38**) and prucalopride (constipation treatment, **39**) were obtained *via* smooth condensation with the amino or hydroxyl groups (Table 3A). These examples demonstrate the compatibility of *N*-PF*t*B secondary amines with various derivatization reactions. Capitalizing on the stability of the N–H bond, we achieved *N*-methylation under strong basic conditions (NaH) using multiple substrates. Naphthalene (**41**), cyano (**40**), benzyl (**42**), ester (**43**), halogen (**44**, **45**), and Boc-protected amino (**46**) substituted *N*-PF*t*B amines yielded the corresponding methylated products in high yields. Interestingly, allyl iodide reacted with compounds **1** and **4** to afford products **47** and **48** (Table 3B), while iodoethane, iodopropane, and iodobutane were unreactive. Additionally, the acylation (**49**) reaction of N–H bond in *N*-PF*t*B secondary amine was successfully performed. Finally, we explored the potential of PF*t*B-labeled molecules for ^{19}F MRI applications using compound **36**. Compared to negative (H_2O) and positive (CF_4) controls, compound **36** exhibited clear imaging sensitivity at various concentrations (25, 50, 75, 100, and 125 mM). Notably, a concentration of 75 mM displayed a high level of discrimination (Table 3C). These findings suggest promising prospects for PF*t*B-labeled secondary amines as ^{19}F MRI contrast agents.

Conclusions

In summary, this study describes a novel and efficient one-step method for the synthesis of aromatic *N*-PF*t*B secondary amines from readily available *N*-CF_3 secondary amine precursors. The reaction involves the strategic elimination of HF from starting materials, rapid conversion of C–F bonds to C-CF_3 groups, and incorporation of the *in situ* generated fluoroform. This method is compatible with a broad range of functional groups, including complex compounds. Experimental results and DFT calculations confirm the involvement of intermediates in the reaction process. This approach not only offers new insights into the reactivity of *N*-CF_3 secondary amines but also provides

a valuable pathway for the development of *N*-PFtB-containing drugs, imaging probes, and contrast agents.

Data availability

The data supporting this article have been included as part of the ESI.†

Author contributions

W. Y. and L. W. conceived the research. L. W. and J. W. carried out all the experiments and data analysis. Z. F. and Z. L. carried out synthesis of various starting materials. Z. G. performed DFT calculations. L. W., J. W. and W. Y. wrote the manuscript with input from all authors.

Conflicts of interest

The authors declare no competing interests.

Acknowledgements

We gratefully acknowledge the National Natural Science Foundation of China (22378205, 22078161), Fundamental Research Funds for the Central Universities (30922010403), Priority Academic Program Development of Jiangsu Higher Education Institutions, the Center for Advanced Materials and Technology in Nanjing University of Science and Technology for financial support.

Notes and references

1 J. Wang, M. Sanchez-Rosello, J. L. Acena, C. del Pozo, A. E. Sorochinsky, S. Fustero, V. A. Soloshonok and H. Liu, *Chem. Rev.*, 2014, **114**, 2432–2506.
2 Y. Zhou, J. Wang, Z. Gu, S. Wang, W. Zhu, J. L. Acena, V. A. Soloshonok, K. Izawa and H. Liu, *Chem. Rev.*, 2016, **116**, 422–518.
3 R. Berger, G. Resnati, P. Metrangolo, E. Weber and J. Hulliger, *Chem. Soc. Rev.*, 2011, **40**, 3496–3508.
4 A. Vitale, R. Bongiovanni and B. Ameduri, *Chem. Rev.*, 2015, **115**, 8835–8866.
5 X. Yang, T. Wu, R. J. Phipps and F. D. Toste, *Chem. Rev.*, 2014, **115**, 826–870.
6 J.-A. Ma and D. Cahard, *Chem. Rev.*, 2008, **108**, PR1–PR43.
7 C. L. Tong, X. H. Xu and F. L. Qing, *Angew. Chem., Int. Ed.*, 2021, **60**, 22915–22924.
8 Q. Wang, Q. Tao, H. Dong, C. Ni, X. Xie and J. Hu, *Angew. Chem., Int. Ed.*, 2021, **60**, 27318–27323.
9 Z. Wei, L. Wen, K. Zhu, Q. Wang, Y. Zhao and J. Hu, *J. Am. Chem. Soc.*, 2022, **144**, 22281–22288.
10 H. Meng, L. Wen, Z. Xu, Y. Li, J. Hao and Y. Zhao, *Org. Lett.*, 2019, **21**, 5206–5210.
11 C. Zhang, K. Yan, C. Fu, H. Peng, C. J. Hawker and A. K. Whittaker, *Chem. Rev.*, 2022, **122**, 167–208.
12 E. Hequet, C. Henoumont, R. N. Muller and S. Laurent, *Future Med. Chem.*, 2019, **11**, 1157–1175.
13 I. Tirotta, V. Dichiarante, C. Pigliacelli, G. Cavallo, G. Terraneo, F. B. Bombelli, P. Metrangolo and G. Resnati, *Chem. Rev.*, 2014, **115**, 1106–1129.
14 K. Tanabe, H. Harada, M. Narazaki, K. Tanaka, K. Inafuku, H. Komatsu, T. Ito, H. Yamada, Y. Chujo, T. Matsuda, M. Hiraoka and S. Nishimoto, *J. Am. Chem. Soc.*, 2009, **131**, 15982–15983.
15 A. Li, X. Luo, D. Chen, L. Li, H. Lin and J. Gao, *Anal. Chem.*, 2023, **95**, 70–82.
16 B. L. Bona, O. Koshkina, C. Chirizzi, V. Dichiarante, P. Metrangolo and F. Baldelli Bombelli, *Acc. Mater. Res.*, 2022, **4**, 71–85.
17 B. Meng, S. L. Grage, O. Babii, M. Takamiya, N. MacKinnon, T. Schober, I. Hutskalov, O. Nassar, S. Afonin, S. Koniev, I. V. Komarov, J. G. Korvink, U. Strähle and A. S. Ulrich, *Small*, 2022, **18**, 2107308.
18 K. Akazawa, F. Sugihara, T. Nakamura, H. Matsushita, H. Mukai, R. Akimoto, M. Minoshima, S. Mizukami and K. Kikuchi, *Angew. Chem., Int. Ed.*, 2018, **57**, 16742–16747.
19 N. G. Taylor, S. H. Chung, A. L. Kwansa, R. R. Johnson, A. J. Teator, N. J. B. Milliken, K. M. Koshlap, Y. G. Yingling, Y. Z. Lee and F. A. Leibfarth, *Chem. Eur. J.*, 2020, **26**, 9982–9990.
20 V. A. Petrov, *Tetrahedron Lett.*, 2000, **41**, 6959–6963.
21 W. J. Middleton and C. G. Krespan, *J. Org. Chem.*, 1965, **30**, 1398–1402.
22 R. J. D. Pasquale, *J. Fluorine Chem.*, 1976, **8**, 311–322.
23 Y. Guo, K. Fujiwara and K. Uneyama, *Org. Lett.*, 2006, **8**, 827–829.
24 J. F. Kögel, L. H. Finger, N. Frank and J. Sundermeyer, *Inorg. Chem.*, 2014, **53**, 3839–3846.
25 Y. L. Yagupolskii and K. I. Petko, *J. Fluorine Chem.*, 2015, **176**, 9–13.
26 L. Wang, J. Wang, S. Ye, B. Jiang, Z. Guo, Y. Mumtaz and W. Yi, *Angew. Chem., Int. Ed.*, 2022, **61**, e202212115.
27 J. X. Xiang, Y. Ouyang, X. H. Xu and F. L. Qing, *Angew. Chem., Int. Ed.*, 2019, **58**, 10320–10324.
28 J. P. Bégué and D. Bonnet-Delpon, *Bioorganic and Medicinal Chemistry of Fluorine*, John Wiley & Sons, Inc., Hoboken, 2008.
29 T. Cheng, Y. Zhao, X. Li, F. Lin, Y. Xu, X. Zhang, Y. Li and R. Wang, *J. Chem. Inf. Model.*, 2007, **47**, 2140–2148.